Available on the CERN CDS information server **CMS PAS HIN-21-007**

CMS Physics Analysis Summary

Contact: cms-pag-conveners-heavyions@cern.ch 2022/04/04

Observation of the Y(3S) meson and sequential suppression of Y states in PbPb collisions at $\sqrt{s_{NN}} = 5.02$ TeV

The CMS Collaboration

Abstract

The production of Y(2S) and Y(3S) mesons in lead-lead (PbPb) and proton-proton (pp) collisions is studied using the CMS detector at the LHC. Their nuclear modification factors, R_{AA}, derived from the ratio of yields measured in PbPb to pp collisions, are reported as functions of transverse momentum and PbPb collision centrality. The Y(3S) meson is observed for the first time in PbPb collisions. The suppression is found to be stronger for Y(3S) mesons compared to Y(2S) mesons, extending the pattern of sequential suppression of bottomonium states in nuclear collisions previously seen for the Y(1S) and Y(2S) states. The results provide new constraints on models describing the dynamics of quarkonium states in heavy ion collisions.

It has been proposed that the yields of quarkonium states are suppressed by Debye screening [1] and by broadening of their widths, both due to interactions with other partons in the QGP [2–5]. These in-medium effects have been studied based on lattice quantum chromodynamics calculations and effective field theories [6, 7]. The screening and broadening of the widths are determined by the real and imaginary parts of the heavy-quark potential, respectively. On the other hand, the yields of quarkonium states can be enhanced in the QGP by both correlated and uncorrelated recombination processes [5–10]. Measurements of bottomonium states in heavy ion collisions have several advantages when studying these in-medium effects. Bottomonia experience the whole evolution of the medium as they are primarily produced at early stages of collisions by hard parton scattering. Furthermore, the number of $\mathrm{q\overline{q}}$ pairs in a single collision event is much smaller for bottom than for charm quarks, and therefore the recombination of uncorrelated quarks is negligible.

Experimentally, the dynamics of quarkonium production in heavy ion collisions are commonly studied using the nuclear modification factor (R_{AA}), which is defined as the ratio of quarkonium yields in nucleus-nucleus (AA) collisions to those in proton-proton (pp) collisions scaled by the average number of binary nucleon-nucleon (NN) interactions in the AA events. The presence of heavy quark potential modification and/or quarkonium recombination has been investigated using measurements of the R_{AA} values at the BNL RHIC and the CERN LHC, both in the charmonium (J/ψ, $\psi(2\mathrm{S})$, χ_{c}, etc.) and bottomonium ($\Upsilon(1\mathrm{S})$, $\Upsilon(2\mathrm{S})$, $\Upsilon(3\mathrm{S})$, χ_{b}, etc.) sectors [11, 12]. The R_{AA} measurements of J/ψ mesons reported by the ALICE Collaboration [13] show that the amount of suppression in the low transverse momentum (p_{T}) region is much weaker at the LHC compared to the results at RHIC. This observation has been successfully described by models incorporating the recombination effects [14, 15].

For bottomonium states, R_{AA} measurements have been reported by the ALICE [16, 17] and CMS Collaborations [18] at LHC, and by PHENIX and STAR Collaborations at RHIC [11]. The results show significant suppression of $\Upsilon(1\mathrm{S})$ mesons in heavy ion collisions, while the $\Upsilon(2\mathrm{S})$ mesons are even more suppressed. The $\Upsilon(3\mathrm{S})$ meson has not yet been observed in AA collisions, but upper limit measurements of R_{AA} (at the 95% confidence level) from the CMS Collaboration using an integrated PbPb luminosity of 368 $\mu\mathrm{b}^{-1}$ are similar to the measured $\Upsilon(2\mathrm{S})$ R_{AA} [18]. Therefore, a larger data sample is needed to examine the relative modification of the Υ excited states and extend the study of the sequential suppression of bottomonium states in heavy ion collisions.

This note reports measurements of the nuclear modification factors for the excited states of bottomonia, $\Upsilon(2\mathrm{S})$ and $\Upsilon(3\mathrm{S})$ mesons, and the double ratios $\Upsilon(3\mathrm{S})/\Upsilon(2\mathrm{S})$ for lead-lead (PbPb) divided by that for pp collisions at a nucleon-nucleon center-of-mass energy of $\sqrt{s_{\mathrm{NN}}} = 5.02\,\mathrm{TeV}$, collected with the CMS detector in 2018 and 2017, respectively. The Υ states are identified using their decay into two oppositely charged muons. The results are presented as functions of the Υ transverse momentum (p_{T}) and the PbPb collision centrality. Centrality is related to the overlap of the two lead nuclei and is defined as the percentage of the total inelastic nucleus nucleus hadronic cross section, with 0% representing the largest overlap [19].

The CMS apparatus [20] is a multipurpose, nearly hermetic detector, designed to trigger on [21, 22] and identify electrons, muons, photons, and (charged and neutral) hadrons [23–26]. A global reconstruction "particle-flow" algorithm [27] combines the information provided by the all-silicon inner tracker and by the crystal electromagnetic and brass-scintillator hadron calorimeters, operating inside a 3.8 T superconducting solenoid, with data from gas-ionization muon detectors interleaved with the solenoid return yoke, to build τ leptons, jets, missing transverse momentum, and other physics objects [28–30]. The forward hadron (HF) calorime-

ters, located at $3 < |\eta| < 5$, extend the pseudorapidity (η) coverage provided by the barrel and endcap detectors. Centrality for PbPb collisions is determined using the sum of the total transverse energy deposited in both of the HF calorimeters.

The events containing Υ mesons are selected using a fast hardware-based trigger system, requiring two muon candidates in a single bunch crossing without explicit requirements on the muon momentum. Additional criteria on the single muon quality and dimuon mass selection are applied in PbPb collisions [31]. The trigger used for pp (PbPb) collisions registered an integrated luminosity of $300\,\mathrm{pb}^{-1}$ ($1.6\,\mathrm{nb}^{-1}$). To reject beam-gas interactions and nonhadronic collisions, an offline event selection is considered [32]. Events are also required to have at least one reconstructed primary vertex. More than 25% of the tracks have to pass a tight track-quality selection for pp collisions [26]. In PbPb collisions, a condition on the compatibility of the silicon pixel detector cluster width [33], and "minimum-bias event" selection determined using the number of towers and energy within the HF detectors [31] are applied. The reconstructed muons are selected using a set of selection criteria [31] to optimize the muon identification. In addition, to ensure high reconstruction efficiency for Υ mesons, the individual muons are required to have $p_{\mathrm{T}} > 3.5$ GeV/c and $|\eta| < 2.4$.

The Monte Carlo (MC) samples for Υ mesons are simulated using PYTHIA 8.212 [34] with the "CP5" tune [35], with the assumption that they are produced unpolarised [36, 37]. Differences of polarization for Υ states in PbPb collisions compared to pp collisions can affect the Υ kinematic distributions, thus requiring different assumptions in the MC simulation at generator level for pp and PbPb collisions. The ALICE Collaboration reported the polarization parameters for $\Upsilon(1S)$ mesons which are found to be consistent with zero [38]. This result suggests the absence of polarization for bottomonium states in PbPb collisions, although there are large uncertainties. The polarization parameters for Υ states in PbPb collisions should be studied in the future with larger statistics. In the MC simulation for PbPb collisions, each Υ event is embedded in a HYDJET 1.9 [39] PbPb event to reproduce the background environment. The MC events are then weighted to match the p_{T} spectra for either pp or PbPb collisions. A full simulation of the CMS detector using GEANT4 [40] is performed to calculate the efficiency. For this analysis, the feed-down contributions, i.e. decays from heavier quarkonium states, are not considered in the MC simulation. The effect of such contributions on the kinematic distribution of the simulated Υ states is included in the reweighting procedure for the p_{T} shape, and, therefore, feed-down should have a small impact on the efficiency factors.

The Υ mesons are reconstructed through the dimuon decay channel, which includes feed-down processes such as decays from P-wave states. The invariant mass of Υ candidates are studied in the 8–14 GeV/c^2 region. In order to reduce the large amount of background in PbPb collisions, signal enriched dimuon candidates are selected in addition using boosted decision trees (BDTs), a multivariate technique algorithm provided by the Toolkit for Multivariate Data Analysis within ROOT [41]. For the BDT training, MC samples and sideband dimuons from the invariant mass spectra in data are used for the signal and background samples, respectively. The dimuons for both data and MC are required to satisfy the overall event and muon selection criteria, while the dimuons in the MC samples must also satisfy the selections used in the online trigger. The training variables for BDT include: the χ^2 probability of the dimuon vertex fit; the distance of closest approach of the Υ meson momentum vector relative to the primary vertex; the distance between the primary vertex and dimuon vertex, both in three dimensions and projected on the transverse plane; the pointing angle, defined as the angle between the line segment connecting the primary and decay vertices and the momentum vector of the reconstructed particle candidates, again in both three dimensions and projected on the transverse plane. The selection is optimized in each studied p_{T} interval. The value of the resulting BDT

variable is selected to maximize the signal significance; $S/\sqrt{S+B}$, where S and B represent the yields for signal and background, respectively.

The yields of Υ states are extracted by an extended unbinned maximum-likelihood fit to the invariant mass distribution. The signal of each Υ state is modeled by a sum of three Crystal-Ball (CB) functions [42]. This choice is made to take into account the different momentum resolution of the muons, which depends on their η. Therefore, the width parameters for the three CB functions are allowed to vary independently, while their mean and radiative-tail parameters are kept the same. The mass parameter of the $\Upsilon(1S)$ state is left free to take into account possible shifts in the calibration of the absolute momentum of the reconstructed tracks. The mean and width parameters for the $\Upsilon(2S)$ and $\Upsilon(3S)$ mesons are the same as found for the $\Upsilon(1S)$ state, but multiplied by the ratio of their PDG world-average masses [43] over the mass of the $\Upsilon(1S)$ meson. All other fit parameters except the yields for the excited states are fixed to those found for the ground state. In fitting the data, all parameters that are used to describe the signal shape except the mean of the $\Upsilon(1S)$ state are constrained to vary within a Gaussian probability density function (PDF). The mean and width of the Gaussian function for each parameter are set to the value and its uncertainty obtained from the fit results on MC samples, respectively. These Gaussian means and widths are found separately for each p_T interval used in the analysis. The background of the mass distribution is modeled using three different functional forms: an error function multiplied by an exponential, a simple exponential, and a Chebyshev polynomial. An Akaike information criterion (AIC) test [44] is performed to determine the nominal function for the background PDF among the three functions. The order of the Chebyshev polynomial is chosen based on a log likelihood ratio test [45].

Figure 1 shows the dimuon invariant mass distributions in pp and PbPb collisions, for the kinematic range $p_T^{\mu^+\mu^-} < 30$ GeV/c and $|y^{\mu^+\mu^-}| < 2.4$, and centrality integrated (0–90%) for PbPb collisions.

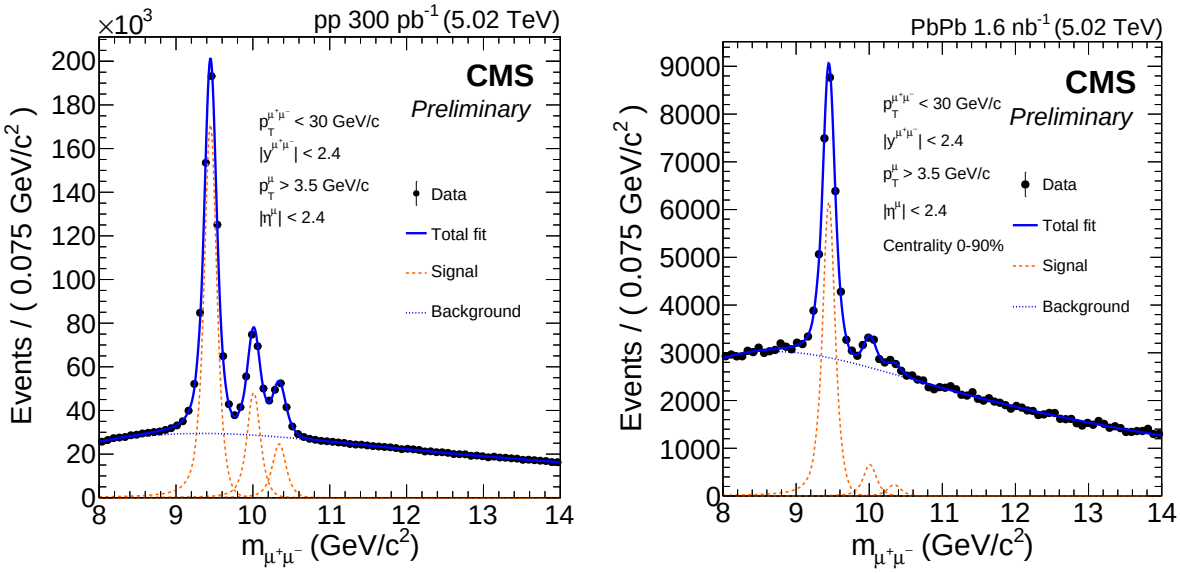

Figure 1: Invariant mass distributions of selected dimuons in pp (left) and PbPb (right) collisions, for the kinematic range $p_T^{\mu^+\mu^-} < 30$ GeV/c and $|y^{\mu^+\mu^-}| < 2.4$. The solid lines in both figures show the results of the fits to data, while the dashed and dotted lines represent the separate yields for each Υ state and background dimuons, respectively.

Acceptance and efficiency correction factors are applied to the extracted number of Υ mesons to

compute the R_{AA} values. Acceptance is defined as the probability for both of the decay muons originating from a Υ meson to be within $p_{\mathrm{T}}^{\mu} > 3.5$ GeV/c and $|\eta^{\mu}| < 2.4$, and is determined using the fraction of MC generated Υ mesons that produce muons in the required kinematic region. The efficiency is calculated using MC and defined as the probability that a dimuon within the acceptance is reconstructed, matched to the trigger, and passes the entire analysis selection criteria. To take into account possible differences between data and MC, the dimuon efficiency is corrected by three components: tracking, identification, and triggering. The efficiency for each individual component is measured using single muons from J/ψ meson decays in both data and MC, with the *tag-and-probe* (T&P) method [46] and applied as a weight for the derivation of the dimuon efficiency.

Table 1: Systematic uncertainties from various sources in pp and PbPb collisions listed in percentage. The global uncertainties are not included in the total uncertainties.

	$\Upsilon(2S)$ (%)		$\Upsilon(3S)$ (%)		$\Upsilon(3S)/\Upsilon(2S)$ (%)	
Source	pp	PbPb	pp	PbPb	pp	PbPb
BDT selection	-	0.3-9.0	-	1.5-18.6	-	1.2-22.8
Background PDF	0.1-1.4	0.3-11.7	0.2-1.6	1.4-21.4	<0.5	0.6-17.6
Signal PDF	0.1-1.1	0.5-2.6	0.4-1.1	0.1-2.5	0.3-0.6	0.1-3.0
Signal parameter	0.1-1.2	0.0-3.8	0.1-1.6	0.3-3.7	0.05-1.4	0.1-0.9
Event selection	-	0.0-0.5	-	0.2-13.1	-	0.1-13.6
Correction factors	<0.1	<0.5	<0.1	<0.4	<2.0	
T&P	0.9-1.0	3.8-4.5	0.9-1.1	3.8-4.4	-	
Total uncertainty	1.0-1.8	3.9-13.5	1.1-2.2	6.0-22.2	0.4-1.5	4.1-23.8

The systematic uncertainties are analyzed for various sources and summarized in Table 1. For each source, the difference of the signal yields in the variation compared to the nominal is taken as the systematic uncertainty. The uncertainty from the signal extraction is considered for three sources: choice of signal parameters, choice of signal PDF, and choice of background PDF. For the parameterization of the signal PDF, the fit results using either the $\Upsilon(2S)$ or $\Upsilon(3S)$ MC samples are used to determine different values for the mean and width of the Gaussian function for each signal parameter. The signal PDF is modified from a sum of three CB functions to a sum of two CB functions and a Gaussian. For the background PDF systematic study, the functions that are rejected in the nominal background PDF determination procedure by the AIC test are used as alternative functions.

The uncertainties from correction factors are also considered. The simulated p_{T} spectra is weighted event by event to match the distribution from data. The acceptance and efficiency values are compared with and without modifying the weighting function by its fit uncertainty. In addition, the uncertainty arising from the T&P correction on single muons is taken into account. The systematic uncertainties in the correction factors of the single muons and the statistical uncertainties coming from the limited size of the data set are propagated to the dimuon efficiency values. The deviations compared to the nominal dimuon efficiencies are summed in quadrature, and assigned as the systematic uncertainty in the T&P correction.

In PbPb collisions, additional uncertainties arise from the BDT training and centrality calibration. To avoid possible biases, the signal and background samples used in BDT training are divided into two and trained independently. Each trained algorithm is applied to the other half of the samples and the average of the two BDT variable values is used as the nominal. The values of each BDT variable are used alternatively and the maximum difference of the corrected

signal yields compared to the nominal is taken as the systematic uncertainty. The centrality calibration is varied by changing the boundaries of the centrality intervals [31] considering the inefficiency in the hadronic event selection.

The total uncertainty is the quadratic sum of all the different sources. Finally, the global uncertainty from collision data is considered. The uncertainty for the integrated pp luminosity is 1.9% [47]. For PbPb data, the uncertainty in counting the minimum-bias collision events sampled by the trigger (N_{MB}) is 1.26% [48]. The overlap function T_{AA} for each PbPb centrality interval is the average number of binary NN collisions per PbPb interaction divided by the inelastic NN cross section, and its uncertainty is estimated by the variation of Glauber model parameters within their uncertainties [49].

The $\Upsilon(3S)$ mesons have been observed for the first time in PbPb collisions with a significance, calculated from the discrete likelihood profiling, above five standard deviations. The nuclear modification factors (R_{AA}) are computed as

$$R_{\mathrm{AA}}(p_{\mathrm{T}}, y) = \frac{N_{\mathrm{AA}}(p_{\mathrm{T}}, y)}{\langle T_{\mathrm{AA}} \rangle \sigma^{\mathrm{pp}}(p_{\mathrm{T}}, y)}, \tag{1}$$

where N_{AA} is the efficiency and acceptance corrected normalized yield of Υ mesons in PbPb collisions, and σ^{pp} is the pp cross section in a given kinematic range. The average value of T_{AA} computed in each centrality bin is denoted by $\langle T_{\mathrm{AA}} \rangle$.

The R_{AA} values for $\Upsilon(2S)$ and $\Upsilon(3S)$ mesons together with the previous measurements for $\Upsilon(1S)$ mesons [18] are presented as functions of $\langle N_{\mathrm{part}} \rangle$ and p_{T} in Fig. 2, where $\langle N_{\mathrm{part}} \rangle$ is the average number of participating nucleons in PbPb collisions for the given centrality interval. A gradual decrease of R_{AA} is observed towards central collisions for both $\Upsilon(2S)$ and $\Upsilon(3S)$ states. On the other hand, a slight increase of R_{AA} is seen with increasing p_{T} for the $\Upsilon(3S)$ state, while no dependence was found for the $\Upsilon(2S)$ state. Both states are found to be strongly suppressed in central PbPb collision events as well as in the overall studied p_{T} region, while the R_{AA} of $\Upsilon(3S)$ is found to be smaller than that of $\Upsilon(2S)$. The R_{AA} values integrated over p_{T} and centrality for $\Upsilon(2S)$ and $\Upsilon(3S)$ are measured to be 0.115 ± 0.008 (stat.) $\pm$ 0.007 (syst.) and 0.080 $\pm$ 0.014 (stat.) $\pm$ 0.012 (syst.), respectively. These results identify the sequential suppression pattern of the bottomonium states in the ordering of their binding energies more clearly than was possible using previous measurements by the ALICE and CMS Collaborations [16, 18].

The double ratio is defined as the yield ratio of $\Upsilon(3S)$ to $\Upsilon(2S)$ in PbPb collisions divided by the same ratio in pp collisions and expressed as

$$\frac{(N_{\Upsilon(3S)} / N_{\Upsilon(2S)})_{\mathrm{PbPb}}}{(N_{\Upsilon(3S)} / N_{\Upsilon(2S)})_{\mathrm{pp}}}, \tag{2}$$

where $N_{\Upsilon(2S)}$ and $N_{\Upsilon(3S)}$ are the measured yields for $\Upsilon(2S)$ and $\Upsilon(3S)$, respectively. The global uncertainties of T_{AA}, pp luminosity, and PbPb N_{MB} are not relevant for the double ratio measurements because of their cancellation in the single ratio $\Upsilon(3S)/\Upsilon(2S)$.

Figure 3 shows the double ratio for $\Upsilon(3S)/\Upsilon(2S)$ as functions of $\langle N_{\mathrm{part}} \rangle$ and p_{T}. The left plot of Fig. 3 shows that the yields for $\Upsilon(3S)$ mesons are more suppressed than those for $\Upsilon(2S)$ mesons towards central PbPb collisions. The double ratios of $\Upsilon(3S)/\Upsilon(2S)$ show no significant dependence on p_{T} as shown in the right plot of Fig. 3.

In summary, data from lead-lead (PbPb) and proton-proton (pp) collisions at a nucleon-nucleon center-of-mass energy of $\sqrt{s_{\mathrm{NN}}} = 5.02$ TeV collected with the CMS detector were analyzed to measure the nuclear modification factors (R_{AA}) of $\Upsilon(2S)$ and $\Upsilon(3S)$ mesons, and double ratios

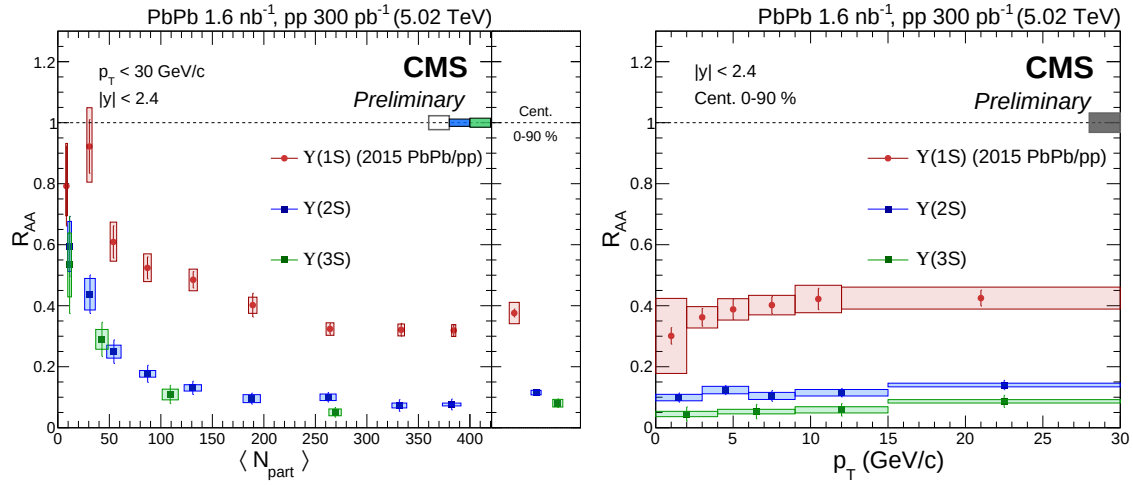

Figure 2: Measured R_{AA} for Υ states as functions of $\langle N_{\mathrm{part}} \rangle$ (left) including the centrality integrated bin and p_{T} (right). The vertical lines correspond to statistical uncertainties, while the boxes represent the systematic uncertainties. In the left figure, the left-most box at unity combines the uncertainties of pp luminosity and PbPb N_{MB}, while the second (third) box corresponds to the uncertainty of pp yields for the $\Upsilon(2\mathrm{S})$ ($\Upsilon(3\mathrm{S})$) state. The box at unity in the right plot combines the uncertainties of T_{AA}, pp luminosity, and PbPb N_{MB}. The results for the $\Upsilon(1\mathrm{S})$ meson are taken from Ref. [18] and are not affected by the boxes at unity.

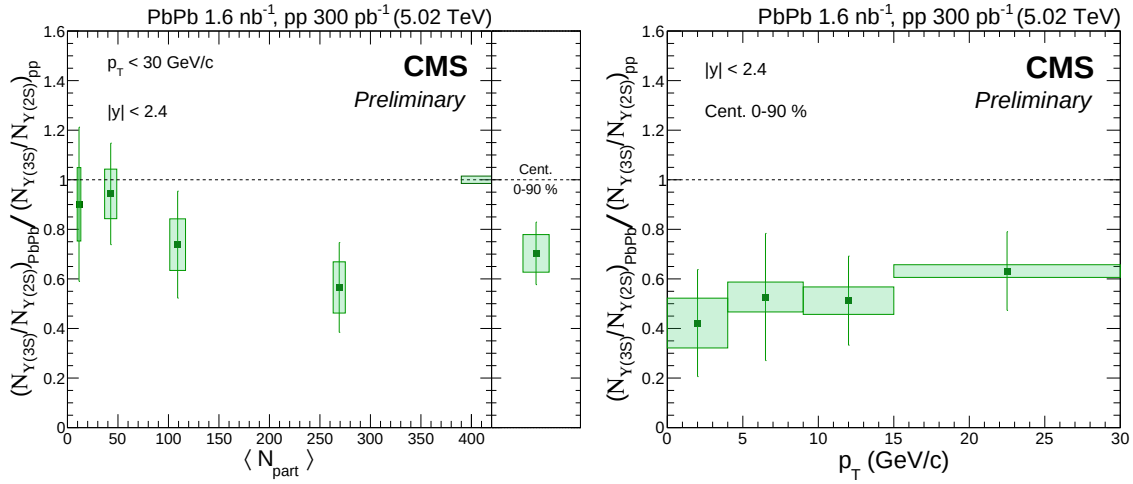

Figure 3: The double ratio of $\Upsilon(3\mathrm{S})/\Upsilon(2\mathrm{S})$ as functions of $\langle N_{\mathrm{part}} \rangle$ (left) and p_{T} (right). The vertical lines correspond to statistical uncertainties, while the boxes are the systematic uncertainties. The box at unity on the left figure shows the combined systematic and statistical uncertainties from pp data, which is common to all of the points.

$\Upsilon(3S)/\Upsilon(2S)$. The values of the observables are given as functions of Υ transverse momentum (p_T) and PbPb collision centrality. The $\Upsilon(3S)$ meson is observed for the first time in PbPb collisions, and the amount of suppression is found to be stronger than for the $\Upsilon(2S)$ meson. The values of R_{AA} for both $\Upsilon(2S)$ and $\Upsilon(3S)$ are observed to decrease gradually for more central collisions. On the other hand, the R_{AA} values suggest at most a small increase with increasing p_T for the $\Upsilon(3S)$ meson. The double ratios are found to be smaller than unity, showing a stronger suppression for the $\Upsilon(3S)$ meson compared to the $\Upsilon(2S)$ meson. No significant p_T dependence is observed for the double ratios $\Upsilon(3S)/\Upsilon(2S)$, indicating the relative modification between the two states to be similar in the studied p_T region. Combined with previous measurements, the results in this note reveal the sequential suppression of $\Upsilon(1S)$, $\Upsilon(2S)$, and $\Upsilon(3S)$ mesons, which provides new constraints on the understanding of quarkonium suppression in heavy ion collisions.

References

[1] T. Matsui and H. Satz, "J/ψ suppression by quark gluon plasma formation", *Phys. Lett. B* **178** (1986) 416, doi:10.1016/0370-2693(86)91404-8.

[2] M. Laine, O. Philipsen, P. Romatschke, and M. Tassler, "Real-time static potential in hot QCD", *JHEP* **03** (2007) 054, doi:10.1088/1126-6708/2007/03/054, arXiv:hep-ph/0611300.

[3] N. Brambilla, J. Ghiglieri, A. Vairo, and P. Petreczky, "Static quark antiquark pairs at finite temperature", *Phys. Rev. D* **78** (2008) 014017, doi:10.1103/PhysRevD.78.014017, arXiv:0804.0993.

[4] N. Brambilla et al., "Heavy quarkonium in a weakly coupled quark-gluon plasma below the melting temperature", *JHEP* **09** (2010) 038, doi:10.1007/JHEP09(2010)038, arXiv:1007.4156.

[5] J.-P. Blaizot, D. De Boni, P. Faccioli, and G. Garberoglio, "Heavy quark bound states in a quark-gluon plasma: Dissociation and recombination", *Nucl. Phys. A* **946** (2016) 49, doi:10.1016/j.nuclphysa.2015.10.011, arXiv:1503.03857.

[6] N. Brambilla et al., "Bottomonium production in heavy-ion collisions using quantum trajectories: Differential observables and momentum anisotropy", *Phys. Rev. D* **104** (2021) 094049, doi:10.1103/PhysRevD.104.094049, arXiv:2107.06222.

[7] X. Yao et al., "Coupled Boltzmann transport equations of heavy quarks and quarkonia in quark-gluon plasma", *JHEP* **01** (2021) 046, doi:10.1007/JHEP01(2021)046, arXiv:2004.06746.

[8] N. Brambilla, M. A. Escobedo, J. Soto, and A. Vairo, "Quarkonium suppression in heavy ion collisions: an open quantum system approach", *Phys. Rev. D* **96** (2017) 034021, doi:10.1103/PhysRevD.96.034021, arXiv:1612.07248.

[9] A. Emerick, X. Zhao, and R. Rapp, "Bottomonia in the quark gluon plasma and their production at RHIC and LHC", *Eur. Phys. J. A* **48** (2012) 72, doi:10.1140/epja/i2012-12072-y, arXiv:1111.6537.

[10] X. Du, R. Rapp, and M. He, "Color screening and regeneration of bottomonia in high-energy heavy-ion collisions", *Phys. Rev. C* **96** (2017) 054901, doi:10.1103/PhysRevC.96.054901, arXiv:1706.08670.

[11] STAR Collaboration, "Suppression of Υ production in dAu and AuAu collisions at $\sqrt{s_{\rm NN}}$=200 GeV", *Phys. Lett. B* **735** (2014) 127, doi:10.1016/j.physletb.2014.06.028, arXiv:1312.3675. [Erratum: doi:10.1016/j.physletb.2015.01.046].

[12] A. Andronic et al., "Heavy flavour and quarkonium production in the LHC era: from proton-proton to heavy ion collisions", *Eur. Phys. J. C* **76** (2016) 107, doi:10.1140/epjc/s10052-015-3819-5, arXiv:1506.03981.

[13] ALICE Collaboration, "Studies of J/ψ production at forward rapidity in PbPb collisions at $\sqrt{s_{\rm NN}} = 5.02$ TeV", *JHEP* **02** (2020) 041, doi:10.1007/JHEP02(2020)041, arXiv:1909.03158.

[14] R. R. Xiaojian Du, "Sequential Regeneration of Charmonia in Heavy-Ion Collisions", *Nuclear Physics A* **943** (2015) 147, doi:10.1016/j.nuclphysa.2015.09.006, arXiv:1504.00670.

[15] Anton Andronic, Peter Braun-Munzinger, Markus K. Köhler, Krzysztof Redlich, Johanna Stachel, "Transverse momentum distributions of charmonium states with the statistical hadronization model", *Phys. Lett. B* **797** (2019) 134836, doi:10.1016/j.physletb.2019.134836, arXiv:1901.09200.

[16] ALICE Collaboration, "Υ suppression at forward rapidity in PbPb collisions at $\sqrt{s_{\mathrm{NN}}}$ = 5.02 TeV", *Phys. Lett. B* **790** (2019) 89, doi:10.1016/j.physletb.2018.11.067, arXiv:1805.04387.

[17] ALICE Collaboration, "Υ production and nuclear modification at forward rapidity in Pb-Pb collisions at $\sqrt{s_{\mathrm{NN}}}$ = 5.02 TeV", *Phys. Lett. B* **822** (2021) 136579, doi:10.1016/j.physletb.2021.136579, arXiv:2011.05758.

[18] CMS Collaboration, "Measurement of nuclear modification factors of $\Upsilon(1S)$, $\Upsilon(2S)$, and $\Upsilon(3S)$ mesons in PbPb collisions at $\sqrt{s_{\mathrm{NN}}} = 5.02\,\mathrm{TeV}$", *Phys. Lett. B* **790** (2019) 270, doi:10.1016/j.physletb.2019.01.006, arXiv:1805.09215.

[19] M. L. Miller, K. Reygers, S. J. Sanders, and P. Steinberg, "Glauber modeling in high energy nuclear collisions", *Ann. Rev. Nucl. Part. Sci.* **57** (2007) 205, doi:10.1146/annurev.nucl.57.090506.123020, arXiv:nucl-ex/0701025.

[20] CMS Collaboration, "The CMS experiment at the CERN LHC", *JINST* **3** (2008) S08004, doi:10.1088/1748-0221/3/08/S08004.

[21] CMS Collaboration, "Performance of the CMS Level-1 trigger in proton-proton collisions at $\sqrt{s} = 13\,\mathrm{TeV}$", *JINST* **15** (2020) P10017, doi:10.1088/1748-0221/15/10/P10017, arXiv:2006.10165.

[22] CMS Collaboration, "The CMS trigger system", *JINST* **12** (2017) P01020, doi:10.1088/1748-0221/12/01/P01020, arXiv:1609.02366.

[23] CMS Collaboration, "Performance of electron reconstruction and selection with the CMS detector in proton-proton collisions at $\sqrt{s} = 8\,\mathrm{TeV}$", *JINST* **10** (2015) P06005, doi:10.1088/1748-0221/10/06/P06005, arXiv:1502.02701.

[24] CMS Collaboration, "Performance of the CMS muon detector and muon reconstruction with proton-proton collisions at $\sqrt{s} = 13$ TeV", *JINST* **13** (2018) P06015, doi:10.1088/1748-0221/13/06/P06015, arXiv:1804.04528.

[25] CMS Collaboration, "Performance of photon reconstruction and identification with the CMS detector in proton-proton collisions at sqrt(s) = 8 TeV", *JINST* **10** (2015) P08010, doi:10.1088/1748-0221/10/08/P08010, arXiv:1502.02702.

[26] CMS Collaboration, "Description and performance of track and primary-vertex reconstruction with the CMS tracker", *JINST* **9** (2014) P10009, doi:10.1088/1748-0221/9/10/P10009, arXiv:1405.6569.

[27] CMS Collaboration, "Particle-flow reconstruction and global event description with the CMS detector", *JINST* **12** (2017) P10003, doi:10.1088/1748-0221/12/10/P10003, arXiv:1706.04965.

[28] CMS Collaboration, "Performance of reconstruction and identification of τ leptons decaying to hadrons and ν_τ in pp collisions at $\sqrt{s} = 13$ TeV", *JINST* **13** (2018), no. 10, P10005, doi:10.1088/1748-0221/13/10/P10005, arXiv:1809.02816.

[29] CMS Collaboration, "Jet energy scale and resolution in the CMS experiment in pp collisions at 8 TeV", *JINST* **12** (2017) P02014, doi:10.1088/1748-0221/12/02/P02014, arXiv:1607.03663.

[30] CMS Collaboration, "Performance of missing transverse momentum reconstruction in proton-proton collisions at $\sqrt{s} = 13$ TeV using the CMS detector", *JINST* **14** (2019) P07004, doi:10.1088/1748-0221/14/07/P07004, arXiv:1903.06078.

[31] CMS Collaboration, "Meaurement of the azimuthal anisotropy of $\Upsilon(1S)$ and $\Upsilon(2S)$ mesons in PbPb collisions at $\sqrt{s_{NN}} = 5.02$ TeV", *Phys. Lett. B* **819** (2021) 136385, doi:10.1016/j.physletb.2021.136385, arXiv:2006.07707.

[32] CMS Collaboration, "Charged-particle nuclear modification factors in PbPb and pPb collisions at $\sqrt{s_{NN}} = 5.02$ TeV", *JHEP* **04** (2017) 039, doi:10.1007/JHEP04(2017)039, arXiv:1611.01664.

[33] CMS Collaboration, "Transverse momentum and pseudorapidity distributions of charged hadrons in pp collisions at $\sqrt{s} = 0.9$ and 2.36 TeV", *JHEP* **02** (2010) 041, doi:10.1007/JHEP02(2010)041, arXiv:1002.0621.

[34] T. Sjöstrand et al., "An introduction to PYTHIA 8.2", *Comput. Phys. Commun.* **191** (2015) 159, doi:10.1016/j.cpc.2015.01.024, arXiv:1410.3012.

[35] CMS Collaboration, "Extraction and validation of a new set of CMS PYTHIA8 tunes from underlying event measurements", *Eur. Phys. J. C* **80** (2020) 4, doi:10.1140/epjc/s10052-019-7499-4, arXiv:1903.12179.

[36] LHCb Collaboration, "Measurement of the Υ polarizations in pp collisions at $\sqrt{s} = 7$ and 8TeV", *JHEP* **12** (2017) 110, doi:10.1007/JHEP12(2017)110, arXiv:1709.01301.

[37] CMS Collaboration, "Measurement of the $\Upsilon(1S)$, $\Upsilon(2S)$, and $\Upsilon(3S)$ polarizations in pp collisions at $\sqrt{s} = 7$ TeV", *Phys. Rev. Lett.* **110** (2013) 081802, doi:10.1103/PhysRevLett.110.081802, arXiv:1209.2922.

[38] ALICE Collaboration, "First measurement of quarkonium polarization in nuclear collisions at the LHC", *Phys. Lett. B* **815** (2021) 136146, doi:10.1016/j.physletb.2021.136146, arXiv:2005.11128.

[39] I. P. Lokhtin et al., "Heavy ion event generator HYDJET++ (hydrodynamics plus jets)", *Comput. Phys. Commun.* **180** (2009) 779, doi:10.1016/j.cpc.2008.11.015, arXiv:0809.2708.

[40] GEANT4 Collaboration, "GEANT4—a simulation toolkit", *Nucl. Instrum. Meth. A* **506** (2003) 250, doi:10.1016/S0168-9002(03)01368-8.

[41] H. Voss, A. Höcker, J. Stelzer, and F. Tegenfeldt, "TMVA, the toolkit for multivariate data analysis with ROOT", in *XIth International Workshop on Advanced Computing and Analysis Techniques in Physics Research (ACAT)*, p. 40. 2007. arXiv:physics/0703039. [PoS(ACAT)040]. doi:10.22323/1.050.0040.

[42] M. J. Oreglia, "A study of the reactions $\psi(2S)' \to \gamma\gamma\psi(2S)$". PhD thesis, Stanford University, 1980. SLAC Report R-236 p.184.

[43] Particle Data Group Collaboration, "Review of Particle Physics", *PTEP* **2020** (2020), no. 8, 083C01, doi:10.1093/ptep/ptaa104.

[44] H. Akaike, "A new look at the statistical model identification", *IEEE Transactions on Automatic Control* **19** (1974) 716, doi:10.1109/TAC.1974.1100705.

[45] M. S. Barlett, "Tests of significance in factor analysis", *British Journal of Statistical Psychology* **3** (1950) 77, doi:10.1111/j.2044-8317.1950.tb00285.x.

[46] CMS Collaboration, "Performance of the CMS muon trigger system in proton-proton collisions at $\sqrt{(}s) = 13$", *JINST* **16** (2021) P07001, doi:10.1088/1748-0221/16/07/p07001, arXiv:2102.04790.

[47] CMS Collaboration, "Luminosity measurement in proton-proton collisions at 5.02 TeV in 2017 at CMS", CMS Physics Analysis Summary CMS-PAS-LUM-19-001, 2021.

[48] CMS Collaboration, "Fragmentation of jets containing a prompt J/ψ meson in PbPb and pp collisions at $\sqrt{s_{\mathrm{NN}}} = 5.02\,\mathrm{TeV}$", *Phys. Lett. B* **825** (2022) 136842, doi:10.1016/j.physletb.2021.136842, arXiv:2106.13235.

[49] C. Loizides, J. Kamin, and D. d'Enterria, "Improved Monte Carlo Glauber predictions at present and future nuclear colliders", *Phys. Rev. C* **97** (2018) 054910, doi:10.1103/PhysRevC.97.054910, arXiv:1710.07098.